

Semi-finished powder of aluminum matrix composite for a direct energy deposition additive manufacturing

JEDYNAK Angelika^{1,a,*}, ERTUGRUL Gökhan^{1,b}, NEUMANN Andreas^{1,c},
PIPPIG Robert^{2,d} and HÄRTEL Sebastian^{1,e}

¹Chair of Hybrid Manufacturing, Brandenburg University of Technology, Cottbus, Germany

²CMMC GmbH, Chemnitz, Germany

^aAngelika.Jedynak@b-tu.de, ^bGökhan.Ertugrul@b-tu.de, ^cAndreas.Neumann@b-tu.de,

^drobert.pippig@cmmc-engineering.com, ^eSebastian.Haertel@b-tu.de

Keywords: Aluminum-Matrix Composites (AMCs), Direct-Vacuum-Casting (DVC), Direct Energy Deposition (DED), Additive Manufacturing (AM)

Abstract. Aluminum-Matrix Composites (AMCs) are particle-reinforced aluminum matrix composites that are well-established in high-performance lightweight components in the automotive and aerospace industries. So far, the use of AMC materials has been limited to components manufactured using casting technology (e.g. brake discs). The adaption of AMC materials in Additive Manufacturing (AM) processes, such as powder feedstock for Direct Energy Deposition (DED), is dependent on the availability of the corresponding semi-finished product. An approach for the production of such a semi-finished product is presented in the current work. This study presents, how powder as semi-finished product for the DED processes, is produced from cast ingots manufactured by Direct-Vacuum-Casting (DVC). The novel DVC process allows a SiC_P particle content of up to 35%, whereas conventional AMC casting processes can only achieve a fully embedded SiC_P particle content of up to 20%. Particular attention is paid to ensuring that the SiC_P particles remain completely embedded in the aluminum matrix after the semi-finished product has been produced. However, there is currently not an extensive literature existing on semi-finished products from AMC materials in AM processes. Therefore, in these investigations, ultrasonic atomization technology was used to produce of AMC powder with an average size of 80 µm as a feedstock material. The microstructure analysis of this powder demonstrated the presence of primary SiC_P particles with non-optimal distribution. Nevertheless, the AMC powder was used in the subsequent DED process studies. It was possible to develop the fundamentals for the deposition processing of AMC powder. As demonstrated by microscope techniques, secondary SiC_P particles were precipitated in an aluminum matrix with complete embedding during deposition, pointing the way forward to develop AMC powders as semi-finished products in AM processes.

Introduction

Aluminum matrix composites (AMCs) are composed of two material systems situated in one material. The aluminum alloy represents a matrix that utilizes low density and corrosion resistance. Ceramics are a possible reinforcement component of the hardness and wear resistance. Due to this unique combination of properties, AMCs are pertinent in various industrial sectors, such as the automotive and aerospace industries [1]. Conventionally, solid or liquid processing routes are available to produce AMC parts, such as sintering, stir casting, and squeeze casting [2]. These processes enable the production of AMC parts with completely embedment and an even distribution of ceramic particles in the matrix. The performance of AMC parts can be further enhanced by increasing the fraction of ceramic particles in the matrix. Therefore, the novel casting processes as Direct-Vacuum-Casting (DVC) allow a SiC_P particle content of up to 35%, whereas



conventional AMC casting processes can only achieve a fully embedded SiC_P particle content of up to 20% [3]. However, the disadvantages of conventional processes are high tooling costs, limited component geometry, and size. Therefore, AM technologies are currently being developed, enabling the production of AMC components without the tooling and lead-time required in conventional processes [4].

The processing of AMCs using AM is still in the initial stage due to the lack of technologies to produce feedstock materials, especially AMC powders. The appropriate morphology, size, and chemical composition of AMC powders are crucial for the AM technologies, such as Laser Powder Bed Fusion (L-PBF) or Direct Energy Deposition (DED), to obtain fully dense components. Also, the uniform distribution of the reinforcement phase within/around the alloy powder particles is significant to achieve the desired mechanical performance of AMC components. The available methods to fabricate AMC powders are ball milling [5] or gas atomization [6]. During the ball milling, AMC powders arise mechanically by the collision of powder particles. The powders produced by this method exhibit, e.g. less sphericity and a mismatch between the reinforcement and the matrix. The more desirable approach to fabricating AMC powders is gas atomization, where the initial material is melted in a crucible and then sprayed by high-pressurized gas jets. This method ensures the production of spherical AMC powders with a uniform distribution of ceramic particles in the matrix. However, a prerequisite to fabricating such powders is a sufficiently long homogenization (by separately added ceramic particles) during melting to avoid segregation. Therefore, using a previously homogenized AMC material, e.g. by a novel DVC, could reduce the processing time of powder production and ensure good powder properties.

The current work presents an approach to the production of AMC powder. An AlSi9Mg aluminum alloy reinforced with 20 vol% SiC_P particles (SiC_P/AlSi9Mg) was considered. The initial material SiC_P/AlSi9Mg was manufactured by DVC and then atomized into SiC_P/AlSi9Mg powder using a novel ultrasonic atomization (UA) technology. In subsequent DED process studies, it was possible to develop the fundamentals for the deposition processing of SiC_P/AlSi9Mg powder. The microstructure evolution of SiC_P/AlSi9Mg powder and as-deposited SiC_P/AlSi9Mg material were investigated using different microscope techniques to determine the presence of SiC_P particles and their embedment behavior in the matrix.

Material and methods

Initial material.

AlSi9Mg aluminum alloy reinforced with 20 vol% SiC_P particles (SiC_P/AlSi9Mg) manufactured by the DVC process [3] was used in this work. The average size of SiC_P was 9.3 μm (=F600). The chemical composition of the aluminum matrix AlSi9Mg is listed in Table 1.

Table 1. Chemical composition of AlSi9Mg alloy in [wt.%] according to the EN AC-43300.

Si	Mg	Fe	Cu	Mn	Zn	Ti	Pb	Al	Others
9.0 - 10.0	0.25 – 0.45	<0.19	<0.05	<0.1	<0.07	<0.15	<0.03	Balance	0.1

Powder fabrication.

The SiC_P/AlSi9Mg powder was produced in the company 3DLab on the ATOLab+ machine using UA technology. In this method, the feed rods are gradually melted by the welding arc, creating a melt pool on the vibrating platform. The droplets are separated from the melt pool by ultrasonic vibrations and discharged by the inert gas flow. During the discharging stage, the formed droplets are solidified leading to the production of powder particles. The atomization process of investigated material was carried out in an atmosphere of pure argon (>99.998%) with a flow rate of 15 – 20 Lmin⁻¹. A significant process parameter was the vibration frequency of 35 kHz, the

amplitude of 80%, and the arc current of 130 A. Finally, the atomized SiC_p /AlSi9Mg powder was sieved with a mesh size of 100 μm.

Specimen manufacturing.

DED is performed with a laser metal deposition (LMD) system, Lunovu e-LMD. The LMD system consists of a 2.5 kW solid state laser power source, a coaxial nozzle corresponding powder feed unit, a 5-axis kinematics and a scanner (see Fig. 1). Laser wavelength and spot diameter are 960 – 1080 nm and 1.6 mm, respectively. Argon is used as a shielding gas with a 12 Lmin⁻¹ flow rate to avoid the atmospheric contamination. The nozzle uses a 3 Lmin⁻¹ powder gas flow rate to carry the powder to the melt pool. Substrate – nozzle distance is 13 mm to focus the laser and powder, simultaneously. The rotation of substrate is chosen between 5 – 10° angle to prevent the reflection (see Fig. 1b).

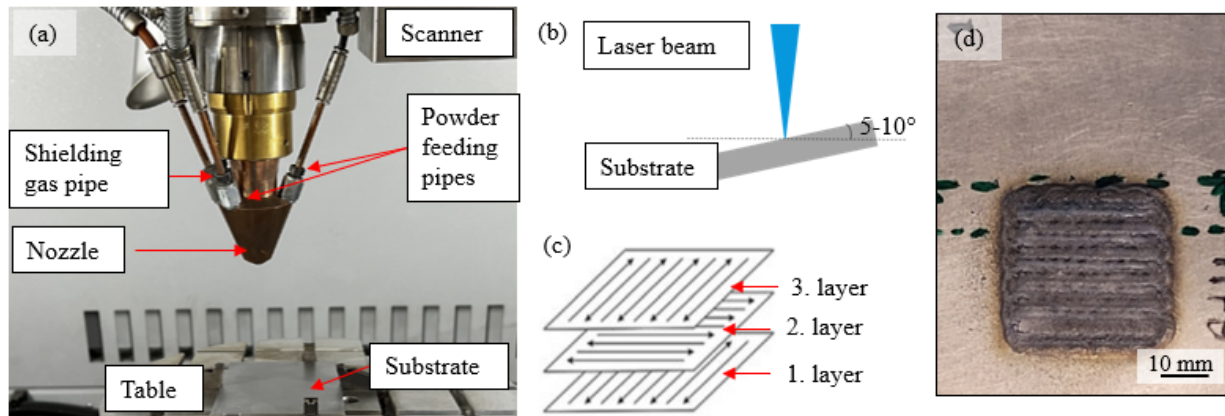


Fig. 1. (a) LMD system components, (b) demonstration of the rotation of substrate and (c) deposition strategy of the additively manufactured part.

The cuboid (length 30 mm, width 30 mm, high 2 mm) was deposited with a bidirectional scanning strategy (with a rotation of 90° to the scanning direction) (see Fig. 1c). The process parameters for the deposition of this part are listed in the Table 2. The distance between parallel track lines was defined as the hatch distance and was approximately 1.7 mm. The number of layers was 6. The overview of the additively deposited part is presented in Fig. 1d.

Table 2. Parameter setup for the manufacturing of the cuboid by DED process.

Laser Power, [W]	Scan Speed, [mms ⁻¹]	Powder feed rate, [gmin ⁻¹]
1750 (1. Layer)	500	1.3
1800 (Upper Layers)		

Powder analysis.

To investigate the morphology (=sphericity) and distribution size of powder particles, scanning electron microscope (SEM) (Phenom XL, Thermofisher Scientific), equipped with a Secondary Electron (SE) detector was used. The imaged powder particles were analyzed with the integrated software ParticleMetric in the SEM to determine the distribution size and sphericity, represented as aspect ratio. The aspect ratio is an index for sphericity, where an aspect ratio of 1 equates to ideal powder sphericity. Approximately, one hundred powder particles were analysed.

For the microstructure analysis, the powder particles were ground using silicon carbide grinding papers with 1200 grit size and oxide polished (0.05 μm silica solution, Struers OP-S Suspension) using a vibratory polishing machine. The Digital Microscope (DM) VHX-7000 (Keyence Deutschland GmbH) was used to investigate the presence, size, morphology, and embedment behaviour of particles in the matrix of powder particles. The size of the particles was measured

with the integrated software in the DM on approximately 25 particles. The chemical composition of particles was measured by SEM using the energy-dispersive X-ray spectrometer (EDX) to determine their type.

Analysis of as-deposited specimen.

To investigate the porosity and microstructure of the as-deposited specimen, the cuboid was sectioned lengthwise to the deposited direction. The sectioned sample of this cuboid was then ground on silicon carbide grinding papers with grit sizes from 240 to 2500, polished using three steps diamond suspension (6 μm , 3 μm and 1 μm), and oxide polished (0.05 μm silica solution, Struers OP-S Suspension). The determination of porosity was carried out using the integrated software in the DM. The microstructure analysis of the as-deposited specimen was carried out in the same way as in the case of powder.

Results and discussion

Initial material.

SEM image of initial microstructure of as-cast $\text{SiC}_p/\text{AlSi9Mg}$ is presented in Fig. 2. This microstructure exhibited a uniform distribution of SiC_p (primary) particles in the aluminum-based matrix.

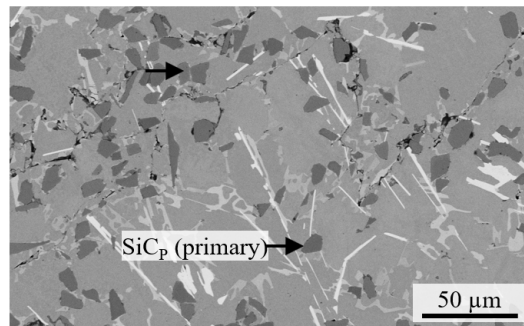


Fig. 2. SEM BSE image of initial microstructure of as-cast $\text{SiC}_p/\text{AlSi9Mg}$.

Powder analysis.

SEM SE image of powder particles of $\text{SiC}_p/\text{AlSi9Mg}$ is shown in Fig. 3 a. The powder particles were spherical and free of satellite particles. The size distribution and the aspect ratio (=sphericity) of powder particles in cumulative frequency are depicted in Fig. 3 b,c. The results have shown that the average size (d_{50}) of powder particles was 80 μm . The particle size distribution (between d_{10} and d_{90}) ranged between 63 μm and 92 μm that was suitable for DED process. The powder particles exhibited very good sphericity, only 10 % of all particles had an aspect ratio below 0.98 (d_{10}) (see Fig. 3 c).

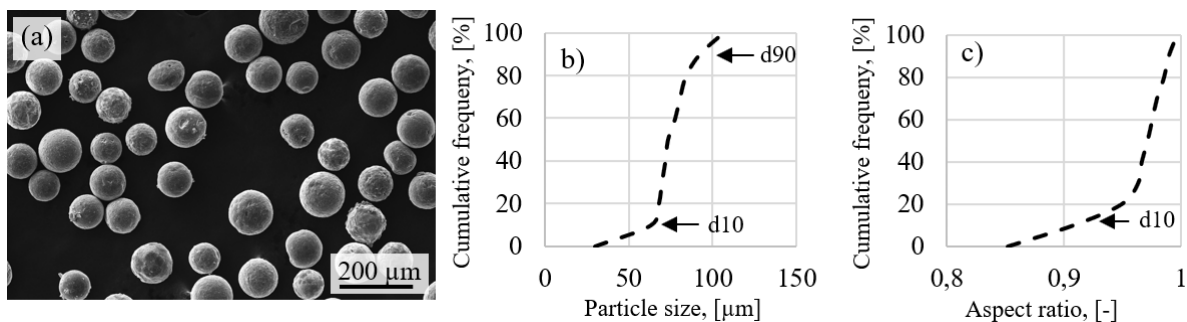


Fig. 3. (a) SEM SE image, (b) particle size distributions and (c) aspect ratio of $\text{SiC}_p/\text{AlSi9Mg}$ powder.

DM images of powder particles of SiC_P/AlSi9Mg in cross-sections are presented in Fig. 4. The powder particles exhibited three predominant types of particles. Their chemical composition was locally determined using EDX analysis (see Table 3), indicating the presence of SiC_P (primary), Al-Si-C and Al-C particles.

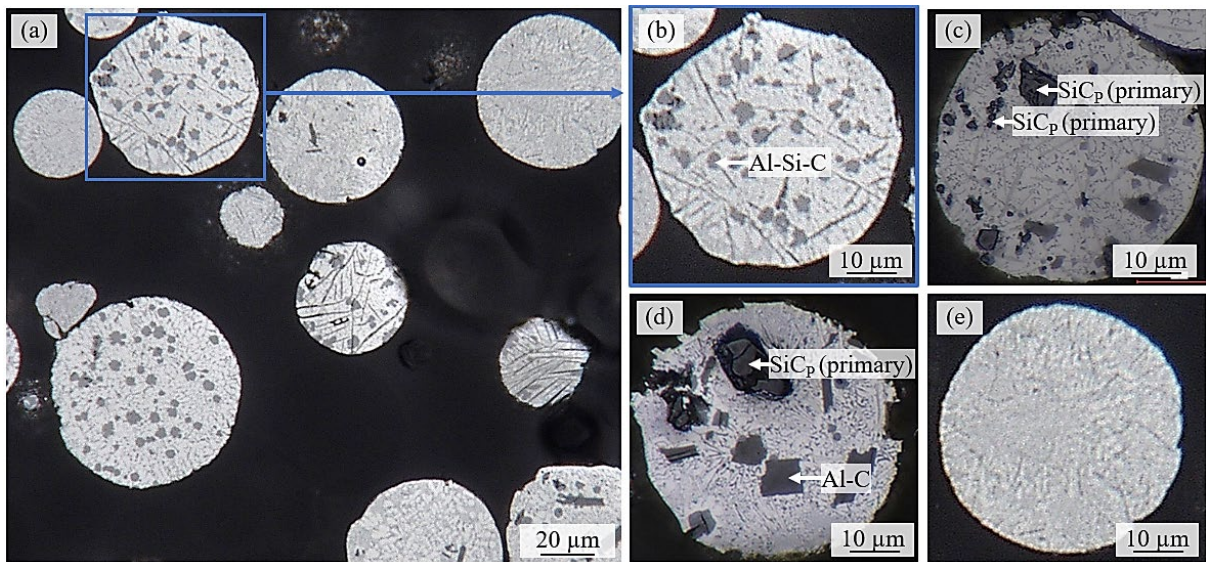


Fig. 4. DM images of particles of SiC_P/AlSi9Mg powder in cross-section.

The similar morphology of the detected SiC_P particles in the powder particles, such as in the initial material, suggests that these particles exhibited resistance during welding arc melting (atomization process) and were transferred into the powder without re-melting. Therefore, the SiC_P in powder particles were determined as primary. However, their average size decreased from 9.2 μm (as-cast) to 4.5 μm (powder), which indicates their partial dissolution. Some primary SiC_P particles had internal cracks due to high thermal stress during the rapid solidification of droplets into powder particles. Furthermore, voids were formed at the interface between these SiC_P particles and the aluminum-based matrix, indicating the non-optimal embedment of these SiC_P particles in the matrix. The presence of primary SiC_P particles was not determined in every particle, indicating their non-uniform distribution in powder particles. The Al-Si-C particles were formed by the reaction of molten aluminum alloy and SiC_P particles [7,8]. The average size of these particles was 8.5 μm. Al-C particles were formed by the similar reaction, depending on the different local temperature and composition [7]. The low oxygen content in these particles indicates their reaction with oxide layer Al₂O₃ on the surface of initial material [9]. Moreover, some powder particles were formed without any precipitated particles.

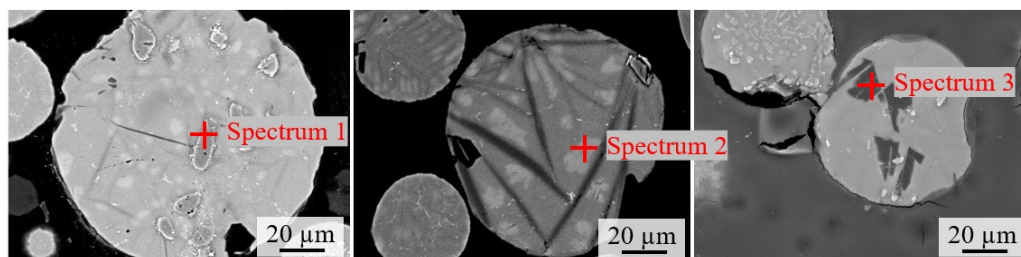


Fig. 5. SEM BSE images of particles of SiC_P/AlSi9Mg powder in cross-section.

Table 3. Chemical composition (at.%) of phases in the microstructure of SiC_P /AlSi9Mg powder.

Spectrum	C	Al	Si	O
Spectrum 1: SiC _P (primary)	49.5	1.5	49.0	--
Spectrum 2: Al-Si-C	37.8	17.0	45.2	--
Spectrum 3: Al-C	79.4	12.3	2.8	5.5

Analysis of as-deposited specimen.

The internal porosity of the as-deposited cuboid is 6.0%, and the pore size ranges between 5 μm to 120 μm. The formation of such high porosity in the as-deposited samples indicates the contamination issues as the result of moisture uptake in aluminum powders [10] or oxygen trapped in SiC_P particles powders processed by atomization process. Nevertheless, the as-deposited SiC_P /AlSi9Mg material was used for the analysis to investigate the presence, morphology and chemical composition of SiC_P particles and their embedment behavior in the matrix.

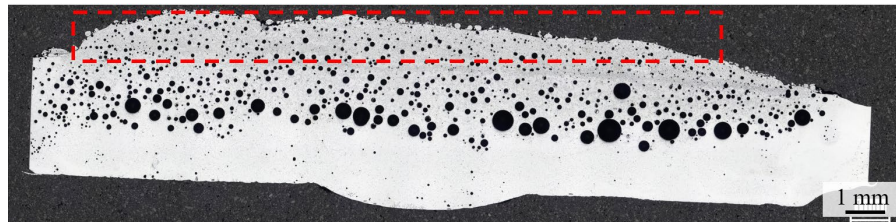


Fig. 6. DM image of the as-deposited cuboid from SiC_P /AlSi9Mg in the longitudinal section.

The microstructure of as-deposited cuboid consisted of uniformly distributed and well-embedded particles in the aluminum alloy matrix. The microstructure from different areas within this part was found to have similar characteristics (see Fig. 7). However, the size of particles was finer at the bottom of the part (Fig. 7 c) as compared to the top/center and edge (Fig. 7 a,b).

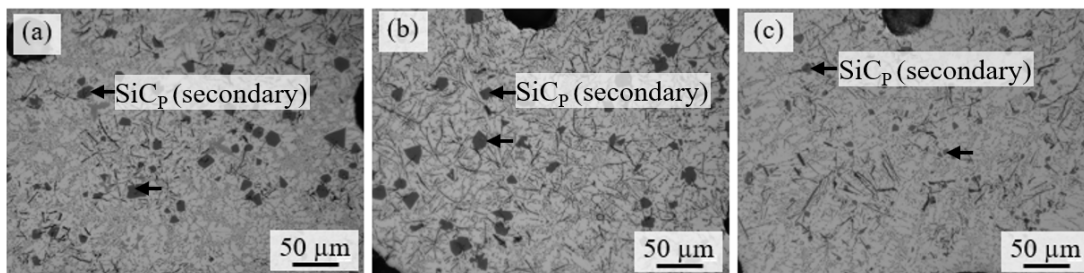


Fig. 7. DM images of microstructure of as-deposited cuboid from SiC_P /AlSi9Mg: (a) at the edge, (b) at the top/centre and (c) at the bottom/centre.

The microstructure of as-deposited cuboid exhibited two predominant types of particles. Their chemical composition was locally determined using EDX analysis (see Table 4), indicating the presence of SiC_P and needle-like Al-Si-C particles (see Fig. 8). The size of the SiC_P was between 22 and 26 μm at the top of the part and 13 μm at the bottom. The shape of these particles was almost angular. Compared to SiC_P (primary) in powder particles, the SiC_P particles in the as-deposited part exhibited a different morphology (larger size and almost angular shape) and were uniformly distributed. That indicates the formation of these SiC_P particles during deposition via mechanism of complete dissolution of powder structure (e.g. primary SiC_P) and their precipitation. Therefore, the SiC_P in powder particles were determined as secondary. The in-situ formation of

SiC_P is thermodynamically possible and can result from the reaction of e.g. Al-C with Si in the melt [7]. In addition, needle-like Al-Si-C particles were formed and uniformly distributed in the microstructure of the as-deposited part. The oxygen content in these particles indicates their reaction with oxide layer Al_2O_3 on the surface of powder particles [9].

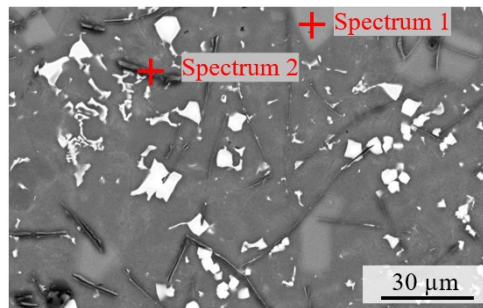


Fig. 8. SEM BSE image of as-deposited cuboid from $\text{SiC}_P / \text{AlSi9Mg}$ (top/centre).

Table 4. Chemical composition (at.%) of the measured spectrums in the microstructure of as-deposited cuboid from $\text{SiC}_P / \text{AlSi9Mg}$ (top/centre).

Spectrum	C	Al	Si	O
Spectrum 1: SiC_P (secondary)	36.1	1.8	60.3	--
Spectrum 2: Al-Si-C	9.6	53.2	9.2	28.0

Conclusions and outlook

In this work, $\text{SiC}_P / \text{AlSi9Mg}$ powder was produced via ultrasonic atomization technology from the $\text{SiC}_P / \text{AlSi9Mg}$ manufactured by the DVC process. The produced $\text{SiC}_P / \text{AlSi9Mg}$ powder was then processed in the DED process. The investigations of the $\text{SiC}_P / \text{AlSi9Mg}$ powder and as-deposited $\text{SiC}_P / \text{AlSi9Mg}$ material with the focus on the microstructure analysis were carried out. The following conclusions can be drawn:

- The $\text{SiC}_P / \text{AlSi9Mg}$ powder exhibited a particle size distribution between $63 \mu\text{m}$ and $92 \mu\text{m}$ and high sphericity, indicating its suitability for the processing with the DED process.
- In the microstructure of $\text{SiC}_P / \text{AlSi9Mg}$ powder, three predominant particles: SiC_P (primary), Al-Si-C and Al-C were determined. The primary SiC_P particles were not uniformly distributed in powder particles and their embedment in the matrix was non-optimal.
- The porosity of the as-deposited sample from the $\text{SiC}_P / \text{AlSi9Mg}$ powder was 6.0%, indicating moisture uptake in aluminum powders or oxygen trapped in SiC_P particles powders processed by atomization process. Nevertheless, the as-deposited part was used to study the evolution of the microstructure during deposition.
- In the microstructure of the as-deposited $\text{SiC}_P / \text{AlSi9Mg}$ material, two predominant particles were determined: SiC_P and needle-like Al-Si-C. The different morphology (shape, size) of these SiC_P particles compared to the primary SiC_P particles (whether in powder or initial material) suggested their formation via the mechanism of dissolution and precipitation (as secondary SiC_P). The distribution of secondary SiC_P was uniform in the as-deposited material with the well-embedding.

Future work will focus on reducing porosity in the DED-processed $\text{SiC}_P / \text{AlSi9Mg}$ material. Therefore, it is necessary to realize measures, such as drying the powder before the AM process, increasing the control of the gas atmosphere during the atomization process, or ensuring appropriate conditions for powder storage are needed to avoid of powder contamination.

References

- [1] P. Garg, A. Jamwal, D. Kumar, K.K. Sadasivuni, C.M. Hussain, P. Gupta, Advance research progresses in aluminium matrix composites: Manufacturing & applications, *J. Mater. Res. Technol.* 8 (2019) 4924–4939. <https://doi.org/10.1016/j.jmrt.2019.06.028>
- [2] V. Chak, H. Chattopadhyay, T.L. Dora, A review on fabrication methods, reinforcements and mechanical properties of aluminum matrix composites, *J. Manuf. Process.* 56 (2020) 1059–1074. <https://doi.org/10.1016/j.jmapro.2020.05.042>
- [3] Graf Mea. New casting process for the production of AMCs with high volume content of einforced particle phase, *Proceedings 5th IMTC 2021*.
- [4] A. Bandyopadhyay, B. Heer, Additive manufacturing of multi-material structures, *Mater. Sci. Eng. R: Reports* 129 (2018) 1–16. <https://doi.org/10.1016/j.mser.2018.04.001>
- [5] X. Xi, B. Chen, C. Tan, X. Song, J. Feng, Microstructure and mechanical properties of SiC reinforced AlSi10Mg composites fabricated by laser metal deposition, *J. Manuf. Process.* 58 (2020) 763–774. <https://doi.org/10.1016/j.jmapro.2020.08.073>
- [6] X.P. Li, G. Ji, Z. Chen, A. Addad, Y. Wu, H.W. Wang, J. Vleugels, J. Van Humbeeck, J.P. Kruth, Selective laser melting of nano-TiB₂ decorated AlSi10Mg alloy with high fracture strength and ductility, *Acta Mater.* 129 (2017) 183–193. <https://doi.org/10.1016/j.actamat.2017.02.062>
- [7] J. Chen, R. Zhang, B.S. Amirkhiz, H. Gu, Synthesis of In Situ SiC/Graphite/Al Hybrid Composite Coating by Laser Direct Energy Deposition, *Metall. Mater. Trans. A* 53 (2022) 484–502. <https://doi.org/10.1007/s11661-021-06508-x>
- [8] R. Anandkumar, A. Almeida, R. Colaço, R. Vilar, V. Ocelik, J.Th.M. De Hosson, Microstructure and wear studies of laser clad Al-Si/SiC(p) composite coatings, *Surf. Coat. Technol.* 201 (2007) 9497–9505. <https://doi.org/10.1016/j.surfcoat.2007.04.003>
- [9] A. Riquelme, P. Rodrigo, M.D. Escalera-Rodríguez, J. Rams, Corrosion Resistance of Al/SiC Laser Cladding Coatings on AA6082, *Coat.* 10 (2020) 673. <https://doi.org/10.3390/coatings10070673>
- [10] C. Weingarten, D. Buchbinder, N. Pirch, W. Meiners, K. Wissenbach, R. Poprawe, Formation and reduction of hydrogen porosity during selective laser melting of AlSi10Mg, *J. Mater. Process. Technol.* 221 (2015) 112–120. <https://doi.org/10.1016/j.jmatprotec.2015.02.013>